

Probing Large-Angle Correlations with the Microwave Background Temperature and Lensing Cross Correlation

A. Yoho,^{1,2} C. J. Copi,¹ G. D. Starkman,^{1,2} A. Kosowsky,³

¹*CERCA/ISO, Department of Physics, Case Western Reserve University, 10900 Euclid Avenue, Cleveland, OH 44106-7079, USA*

²*CERN, CH-1211 Geneva 23, Switzerland*

³*Department of Physics and Astronomy, University of Pittsburgh, Pittsburgh, PA 15208 USA*

24 March 2022

ABSTRACT

A lack of correlations in the microwave background temperature between sky directions separated by angles larger than 60° has recently been confirmed by data from the *Planck* satellite. This feature arises as a random occurrence within the standard Λ CDM cosmological model less than 0.3 per cent of the time, but so far no other compelling theory to explain this observation has been proposed. Here we investigate the theoretical cross-correlation function between microwave background temperature and the gravitational lensing potential of the microwave background, which in contrast to the temperature correlation function depends strongly on gravitational potential fluctuations interior to our Hubble volume. For standard Λ CDM cosmology, we generate random sky realizations of the microwave temperature and gravitational lensing, subject to the constraint that the temperature correlation function matches observations, and compare with random skies lacking this constraint. The distribution of large-angle temperature-lensing correlation functions in these two cases is different, and the two cases can be clearly distinguished in around 40 per cent of model realizations. We present an *a priori* procedure for using similar large-angle correlations between other types of data, to determine whether the lack of large-angle correlations is a statistical fluke or points to a shortcoming of the standard cosmological model.

1 INTRODUCTION

Observations of the Cosmic Microwave Background (CMB) have provided cosmologists with a wealth of information about our early Universe. On its own, and especially in concert with data from complementary probes, CMB observations have lead to increasingly tight constraints on the inferred values of cosmological parameters, and have allowed us to distinguish among various models of our Universe. This has resulted in a standard cosmological model: inflationary flat Lambda Cold Dark Matter (Λ CDM).

Despite its great successes, Λ CDM has had difficulty explaining certain features in the CMB that were initially characterized by the *Cosmic Background Explorer's Differential Microwave Radiometer (COBE-DMR)* (Bennett et al. 1996; Hinshaw 1996) or using *Wilkinson Microwave Anisotropy Probe (WMAP)* observations (Spergel et al. 2003; Chang & Want 2013; Copi et al. 2007, 2009, 2010) and recently confirmed (Ade et al. 2013; Copi 2013b) with the first release of temperature data from the *Planck* satellite. These features are predominantly in the large-angle, or low ($\ell \lesssim 30$) multipole, regime. The anomalies include an Ecliptic north-south hemispherical asymmetry (Eriksen et al. 2007), the alignment of the quadrupole and octopole patterns with one another (de Oliveria-Costa et al. 2004; Copi et al. 2004; Land & Magueijo 2005; Copi et al. 2013 in preparation), with the Ecliptic (Schwarz et al. 2004) and with the cosmological

dipole (Copi et al. 2006), and low variance across the sky (Hou, Banday & Gorski 2009). A full list as well as comparison to *WMAP* observations can be found in (Ade et al. 2013).

Another large-angle anomaly, namely the lack of correlation on the CMB sky at angles larger than about 60° , currently has no compelling explanation. The importance of this feature has been outlined in papers over the last several years (Schwarz et al. 2004). Thus far, this anomaly has been observed only in the temperature auto correlation function. There has been some suggestion that it is merely a statistical fluke (which we call the fluke hypothesis, or the null hypothesis because it is just standard cosmology informed by the experimental data) especially since it was only noted and characterized *a posteriori*. Moreover, it will be difficult to improve on the current statistical significance purely through further observation of the temperature correlations because of cosmic variance and because the measurements are statistics limited.

The use of temperature data exclusively is due to to a lack of high signal-to-noise full-sky maps of other cosmological quantities, such as polarization and lensing potential. With the highly anticipated upcoming release of the *Planck* polarization map as well as several upcoming lensing experiments, cosmologists will have information on large-angle correlation functions beyond just microwave temperature data. Recently the ability for a temperature- Q polariza-

arXiv:1310.7603v1 [astro-ph.CO] 28 Oct 2013

tion cross correlation to test the fluke hypothesis was investigated (Copi 2013a). The results of that work showed that there was a possibility for TQ correlations to rule out the null hypothesis, but that it would not necessarily be a definitive test. In this work we will investigate the possibility for a cross correlation between temperature and CMB lensing potential to provide a test of the statistical fluke hypothesis as well as a consistency check for observations. We provide predictions for the distribution of a standard statistic used in two-point correlation function analysis, $S_{1/2}$, as well as define an optimal, *a priori* statistic for use with temperature-lensing cross correlations.

While in this paper we present results comparing two particular models – unconstrained and constrained Λ CDM – we use a generic prescription for optimization and for determining the viability of an $S_{1/2}$ -like statistic. This analysis can be repeated for any set of models as long as one knows how to produce realizations within that framework. This reason in particular was a driving force in the choice of unconstrained Λ CDM for our comparison model, as generating realizations is straightforward. With the particular choice of $T\varphi$ correlations, the discriminating power of the $S^{T\varphi}$ statistic will depend on how a particular model suppresses the $\Theta_{\text{ISW}}\varphi$ term in the correlation, as this is the piece that dominates the signal, unlike TT correlations. However, this analysis can *always* be carried out such that the $S_{1/2}$ -like statistic can be optimized *a priori* for correlations between cosmological data sets.

The paper is organized as follows: in Sec. 2 we will give the theoretical background for CMB two-point correlation function analysis, in Sec. 3 we will describe how we generate constrained Λ CDM realizations, in Sec. 4 we will outline our general prescription for calculating statistics, in Sec. 5 we will present our results for the distributions of the statistic for two models (constrained and unconstrained Λ CDM), and finally in Sec. 6 we will summarize and state our conclusions.

2 BACKGROUND

The two-point angular correlation function for the CMB temperature is calculated by taking an ensemble average of the temperature fluctuations in different directions:

$$C^{TT}(\theta) = \langle \Theta(\hat{\mathbf{n}}_1)\Theta(\hat{\mathbf{n}}_2) \rangle \quad \text{with} \quad \hat{\mathbf{n}}_1 \cdot \hat{\mathbf{n}}_2 = \cos\theta. \quad (1)$$

Since we are not able to compute the ensemble average in practice, we instead calculate $\mathcal{C}^{TT}(\theta)$, a sky average over the angular separation. In general, any $C(\theta)$ can be expanded in a Legendre series, which we write as

$$C(\theta) = \sum_{\ell} \frac{\ell(\ell+1)}{4\pi} C_{\ell} P_{\ell}(\cos\theta), \quad (2)$$

where the C_{ℓ} on the right-hand side of Eq. 2 are the measured power spectrum values. On a full sky, the coefficients C_{ℓ} obtained from the estimator

$$C_{\ell} \equiv \frac{1}{2\ell+1} \sum_{m=-\ell}^{\ell} |a_{\ell m}|^2, \quad (3)$$

where the $a_{\ell m}$ are the usual spherical harmonic coefficients of a map, are identical to the C_{ℓ} in Eq. 2. Computationally it is more efficient to use the relations (2) and (3) than to directly correlate pairs of pixels on the observed CMB sky.

The two-point function from the *COBE-DMR*'s fourth-year data release (Bennett et al. 1996) highlighted a lack of temperature auto-correlations for angular separations larger than 60 degrees. The *WMAP* first-year data release (Spergel et al. 2003) first quantified this feature using an (*a posteriori*) statistic that neatly captured the simple observation that $C(\theta)$ nearly vanished at large angles

$$S_{1/2}^{TT} \equiv \int_{1/2}^{-1} d(\cos\theta) [C^{TT}(\theta)]^2. \quad (4)$$

We generalize this to

$$S_{1/2}^{XY} \equiv \int_{1/2}^{-1} d(\cos\theta) [C^{XY}(\theta)]^2, \quad (5)$$

where X, Y can be any combination of cosmological quantities for which $C^{XY}(\theta)$ can be calculated. The *WMAP* team calculated $S_{1/2}^{TT}$ on the most reliable part of the sky – that outside the galactic plane – and found it to be $1152 \mu\text{K}^4$, much smaller than the expected Λ CDM value of $\sim 50\,000 \mu\text{K}^4$. They remarked: ‘For our Λ CDM Markov chains... only 0.15% of the simulations have lower values of S .’

The simplest (and perhaps leading) explanation for this anomaly is that it is just a statistical fluke within completely canonical Λ CDM. In this paper, our goal is to define *a priori* a statistic that can be used with future data to test the fluke hypothesis. We therefore need to find an independent cross correlation that would respond to the same statistical fluctuations as the temperature two-point function. To this end we focus on the lensing of the CMB, and construct the cross correlation, $C^{T\varphi}(\theta)$, between the CMB temperature T and the CMB lensing potential φ . Since both derive from the gravitational potential Φ , we expect that if statistical fluctuations generated by primordial physics in Φ caused the lack of large-angle temperature auto-correlation, then those statistical fluctuations would also imprint themselves in a new, distinct way on $C^{T\varphi}(\theta)$.

Since we know that at large angles the CMB signal is dominated by the Sachs-Wolfe (SW) and Integrated Sachs-Wolfe (ISW) contributions, we can write

$$\Theta(\hat{\mathbf{n}}) = \Theta_{\text{SW}}(\hat{\mathbf{n}}) + \Theta_{\text{ISW}}(\hat{\mathbf{n}}) \quad (6)$$

and can describe $C^{TT}(\theta)$ as a correlation of these two terms only. The SW and ISW pieces of the primordial temperature fluctuations in terms of the metric potential, Φ , are

$$\Theta_{\text{SW}}(\hat{\mathbf{n}}) = -\frac{1}{3}\Phi(\chi\hat{\mathbf{n}}, \chi) \quad (7)$$

and

$$\Theta_{\text{ISW}}(\hat{\mathbf{n}}) = -2 \int_0^{\chi_*} d\chi \dot{\Phi}(\chi\hat{\mathbf{n}}, \chi), \quad (8)$$

which allows us to write $C^{TT}(\theta)$ in terms of correlations of Φ as

$$\begin{aligned} C^{TT}(\theta) &= \frac{1}{9} \langle \Phi(\chi_*\hat{\mathbf{n}}_1, \chi_*) \Phi(\chi_*\hat{\mathbf{n}}_2, \chi_*) \rangle \\ &+ \frac{2}{3} \int d\chi_1 \langle \dot{\Phi}(\chi_1\hat{\mathbf{n}}_1, \chi_1) \dot{\Phi}(\chi_*\hat{\mathbf{n}}_2, \chi_*) \rangle \\ &+ 4 \int d\chi_1 d\chi_2 \langle \dot{\Phi}(\chi_1\hat{\mathbf{n}}_1, \chi_1) \dot{\Phi}(\chi_2\hat{\mathbf{n}}_2, \chi_2) \rangle. \end{aligned} \quad (9)$$

Similarly, we can write the CMB lensing potential φ in

terms of the metric potential,

$$\varphi(\hat{\mathbf{n}}) = 2 \int_0^{\chi_*} d\chi \frac{\chi_* - \chi}{\chi_* \chi} \Phi(\chi \hat{\mathbf{n}}, \chi), \quad (10)$$

which allows us to write an expression for the two-point function of the CMB temperature and lensing field:

$$\begin{aligned} C^{T\varphi}(\theta) &= \langle \varphi(\hat{\mathbf{n}}_1) \Theta_{\text{SW}}(\hat{\mathbf{n}}_2) \rangle + \langle \varphi(\hat{\mathbf{n}}_1) \Theta_{\text{ISW}}(\hat{\mathbf{n}}_2) \rangle \\ &= -\frac{2}{3} \int d\chi_1 \langle \Phi(\chi_1 \hat{\mathbf{n}}_1, \chi_1) \Phi(\chi_* \hat{\mathbf{n}}_2, \chi_*) \rangle \\ &\quad - 4 \int d\chi_1 d\chi_2 \langle \Phi(\chi_1 \hat{\mathbf{n}}_1, \chi_1) \dot{\Phi}(\chi_2 \hat{\mathbf{n}}_2, \chi_2) \rangle, \end{aligned} \quad (11)$$

where computations to find $C^{T\varphi}(\theta)$ from data will use sky averages rather than ensemble averages.

From (11), we see that the lensing field also accesses the information encoded in Φ . Thus, if the anomalous absence of large-angle correlations in $C^{TT}(\theta)$ is due to statistical fluctuations, then it should be present in a predictable way in the $C^{T\varphi}(\theta)$ cross correlation. It should be noted, however, that $C^{T\varphi}(\theta)$ traces the same physics in a different way – the terms Eq. 11 do not exactly match the SW and ISW terms in Eq. 9. Furthermore, $C^{T\varphi}(\theta)$ is dominated by the ISW- φ term, meaning the behavior of the two-point cross correlation is dominated by physics on the interior of our Hubble volume, whereas $C^{TT}(\theta)$ has its largest contribution from the SW-SW term and is therefore dominated by physics at the last scattering surface. This makes $C^{T\varphi}(\theta)$ a complementary probe into the nature of the lack of correlation in $C^{TT}(\theta)$ at large angles.

The way that the cross correlation of the temperature and lensing fields will be affected depends on the underlying details contained in the metric potential. This means that predictions of how $C^{T\varphi}$ will be affected by new physics can only occur after choosing a particular model. Consequently, absent a specific alternative model we cannot construct a statistic that fits well into a Bayesian statistical approach and differentiates between the fluke hypothesis and all other models generically. The approach we therefore take is to use Λ CDM (without the constraints imposed by the fluke hypothesis) as the comparison model for its predictions of the statistical properties of $C^{T\varphi}$ and then construct as $S_{1/2}^{T\varphi}$ -like statistic that optimizes the ability to select between the fluke hypothesis and this comparison model. The statistic we propose can thus be used to falsify the prediction of the fluke hypothesis.

3 CONSTRAINED SKY REALIZATIONS

We know that we live in a Universe with a particular angular power spectrum of the temperature, C_ℓ^{TT} , and a particular value of $S_{1/2}^{TT}$, and we must see what including this as a prior constraint on the allowed realizations of Λ CDM does to the probability distribution of values of our target statistic.

It is well known how to create realizations of ordinary Λ CDM with a fixed set of parameters. It is more unusual to create constrained realizations of Λ CDM – ones that reproduce, within the measurement errors, the angular power spectrum of the observed sky, and with both a full sky and a cut sky $S_{1/2}^{TT}$ no larger than those of the observed sky. A detailed description of how create constrained realizations is contained in section 2 of (Copi 2013a). Briefly, we treat the

observational errors in the *WMAP*-reported C_ℓ^{TT} as Gaussian distributed and generate many random C_ℓ^{TT} from Gaussian distributions centred on the *WMAP*-reported values, and correct this realization for the slight correlation induced on partial skies. The resulting sky realization is guaranteed to have a full-sky $S_{1/2}^{TT}$ consistent with the small value in the full-sky *WMAP* ILC map. We only keep realizations with an $S_{1/2}^{TT}$ less than the observed cut-sky calculated value (1292.6 μK^4 for *WMAP*-7 and 1304 μK^4 for *WMAP*-9) for analysis.

With a set of 10^5 such constrained temperature realizations, $a_{\ell m}^T$, we can compute the corresponding set of constrained lensing potential realizations, $a_{\ell m}^\varphi$. This is done using standard techniques for generating correlated random variables using the HEALPix package¹ (Gorski et al. 2005) and is reviewed in the appendix of (Copi 2013a). The required input spectra $C_\ell^{T\varphi}$ and $C_\ell^{\varphi\varphi}$ were generated with CAMB² (Lewis 1999).

A full-sky analysis of the CMB relies on a reconstruction of the fluctuations behind the Galactic cut. We instead use the cut-sky measured value as a threshold to avoid any bias that the reconstruction might induce. We emphasize that no attempt is made (nor is any necessary) to argue that the cut-sky statistic is a better estimator of the value of some full-sky version of the statistic on the full-sky (if we could measure it reliably) or on the ensemble. The cut-sky statistic need only be taken at face value as a precise prescription for something that can be calculated from the observable sky. Calculating $S_{1/2}$ with partial sky data has a well defined procedure – statistics are just calculated using pseudo- C_ℓ s without reference to any full sky estimators. A more detailed discussion of this can be found in (Copi 2013a).

4 CALCULATING $S_{1/2}$ AND S_X STATISTICS

Once we have a set of $a_{\ell m}^T$ and $a_{\ell m}^\varphi$, we can calculate $S_{1/2}^{T\varphi}$ as above (5). However, instead of using $C(\theta)$ directly, we calculate the statistic using C_ℓ s:

$$S_{1/2}^{XY} \equiv \int_{-1}^{1/2} d(\cos\theta) [C^{XY}(\theta)]^2 = \sum_{\ell=2}^{\ell_{\text{max}}} C_\ell^{XY} I_{\ell\ell'} C_{\ell'}^{XY}. \quad (12)$$

In computing Eq. 12 we used an $\ell_{\text{max}} = 100$, as the C_ℓ fall sharply and higher order modes have a negligible contribution to the statistic. An explicit definition of the $I_{\ell\ell'}$ matrix can be found in Appendix B of (Copi et al. 2009).

For temperature-lensing cross correlations, we can optimize the statistic *a priori* so that it best discriminates between constrained realizations of Λ CDM and unconstrained Λ CDM. To do this, we generalize $S_{1/2}$ to

$$S_{a,b}^{XY} = \int_a^b d(\cos\theta) [C^{XY}(\theta)]^2 \quad \text{for } -1 \leq a < b \leq 1. \quad (13)$$

For each possible pair of $a = \cos(\theta_a)$ and $b = \cos(\theta_b)$, we calculate the distribution of $S_{a,b}^{T\varphi}$ values for ensembles of both constrained and unconstrained realizations. We compute the 99-per centile value for the constrained distribution (i.e. the value of $S_{a,b}^{T\varphi}$ that is greater than 99 per cent of the members of the constrained ensemble). We then determine the fraction of the values in the $S_{a,b}$ distribution for the unconstrained ensemble that are larger than the 99 per cent constrained value. The higher the percentile, the better $S_{a,b}^{T\varphi}$ is at discriminating between the constrained and unconstrained models. We repeat the analysis for 99.9-percentile.

¹ <http://healpix.sourceforge.net>

² <http://camb.info>

We choose two different confidence levels for analysis here to show that optimization will lead to different (a, b) ranges. The confidence level and corresponding percentage for optimization should always be chosen before any analysis on a particular data set is carried out. This process was performed using reported C_ℓ^{TT} and corresponding error bars from both *WMAP* 7- and *WMAP* 9-year releases.³

5 RESULTS

The distributions on a cut sky for unconstrained Λ CDM and for Λ CDM constrained by the *WMAP* 9-year power spectrum and $S_{1/2}^{TT}$ value are shown in Fig. 1. The two distributions have a significant overlap. The analysis shows 39.6 per cent of the unconstrained Λ CDM values fall above the 99-per centile constrained value of $1.48 \times 10^{-7} \mu\text{K}^2$, and 26.7 per cent of the unconstrained Λ CDM values falling above the 99.9-per centile constrained value of $2.47 \times 10^{-7} \mu\text{K}^2$.

We repeated this analysis for the *WMAP* 7-year release, and found a negligible difference between results generated with the 7- and 9-year data sets. We conclude that the changes in *WMAP* reported values and error bars and the best-fitting model for C_ℓ^{TT} by release year do not affect the results in any significant way. We have also calculated all of the generalized $S_{a,b}^{T\varphi}$ statistics for the 7- and 9-year data, and found that it as well produced similar results. Therefore, we will proceed with presenting only the results from the *WMAP* 9-year analysis.

Figs. 2 and 3 show only a small improvement by choosing to integrate over a range of angles other than 60° to 180° . The maximum discriminating power is 40.4 per cent for the statistic integrating over the range $a = \cos(168^\circ)$, $b = \cos(48^\circ)$. For the 99.9-per centile, the maximum discriminating power drops to 27.8 per cent, with the optimal range of angles changing slightly to $a = \cos(127^\circ)$, $b = \cos(53^\circ)$. Figs. 4 and 5 show the distribution of the $S_{a,b}$ statistic from Eq. 13 for these ranges of angle-cosines. The 99-per centile value of the statistic for $\theta_a = 168^\circ$, $\theta_b = 48^\circ$ on the ensemble of constrained realizations is $1.43 \times 10^{-7} \mu\text{K}^2$, and the 99.9-per centile value for $\theta_a = 127^\circ$, $\theta_b = 53^\circ$ is $1.50 \times 10^{-7} \mu\text{K}^2$.

We have not repeated the analysis for the first *Planck* temperature maps because an approximate covariance matrix is not yet available, but we expect the results to be similar based on the close match between large-scale features in the *WMAP* and *Planck* sky maps.

6 CONCLUSIONS

In light of the new data from *Planck*, large-angle anomalies have been gaining more traction in the community as potential evidence of interesting primordial physics that deviates from the widely accepted Λ CDM paradigm. In particular, the observed lack of temperature-temperature correlations at angles larger than 60° has been characterized by the $S_{1/2}^{TT}$ statistic, and the measured value has shown to occur in less than .1 per cent of standard Λ CDM realizations on a 9-year KQ85 masked sky (Copi et al. 2004; Copi 2013b). Since $S_{1/2}^{TT}$ was an *a posteriori* choice of a statistic after seeing the shape of the two-point function from the *WMAP* data, the possibility that our Universe happens to just be a statistical fluke has been advocated. We wish to test this hypothesis by calculating statistics for a different correlation function whose distribution would be expected to be markedly altered (compared to normal) in realizations of Λ CDM that reproduce the observed small $S_{1/2}^{TT}$. For this purpose we have used

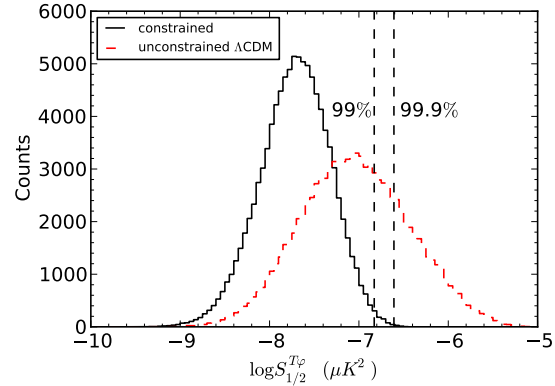


Figure 1. Histogram of $S_{1/2}^{T\varphi}$ values for 10^5 simulations for constrained (black solid) and unconstrained (red dashed) Λ CDM realizations from *WMAP* 9 parameters. The dashed lines show the 99-per centile and 99.9-per centile values for the constrained realizations.

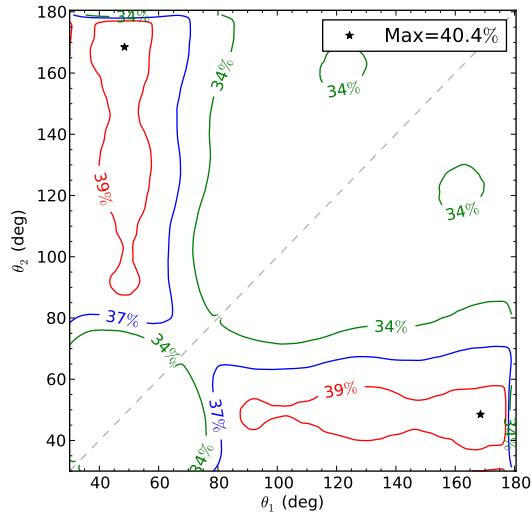


Figure 2. Contour plot showing percentage of unconstrained Λ CDM $S_{a,b}^{T\varphi}$ values falling above the 99-per centile value for the constrained realizations. Stars show the maximum difference, which occurs for an integral over the range of 48° to 168° .

the cross-correlation between temperature and lensing potential φ as an *a priori* test of the null hypothesis.

We have calculated the distribution of the $S_{1/2}^{T\varphi}$ statistic for 10^5 realizations of unconstrained Λ CDM with the *WMAP* 7 and *WMAP* 9 best-fitting cosmological parameters, as well as a similar number of realizations constrained to have a value for $S_{1/2}^{TT}$ no larger than the observed value, and found no significant difference between results calculated from each data set despite changes to the reported central values and error bars. We showed that 39.2 per cent of members of the ensemble of unconstrained realizations had $S_{1/2}^{T\varphi}$ greater than the 99-per centile value of $S_{1/2}^{TT}$ in the ensemble of constrained realizations. This represents a modest (but not insignificant) ability to distinguish strongly between the constrained and unconstrained models.

We have also defined a generalised statistic for testing the

³ <http://lambda.gsfc.nasa.gov/>

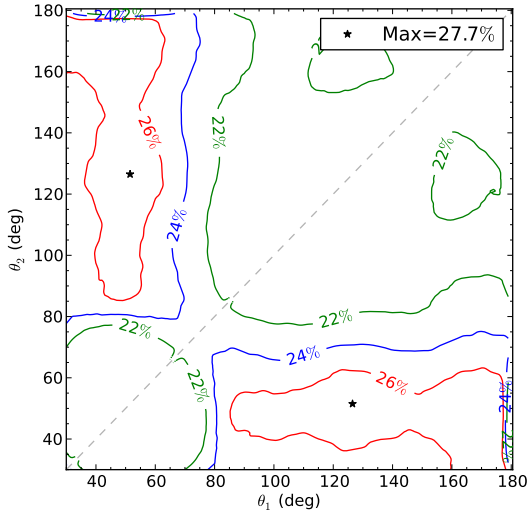


Figure 3. Contour plot showing percentage of unconstrained Λ CDM $S_{a,b}^{T\varphi}$ values falling above the 99.9-per centile value for the constrained realizations. Stars show the maximum difference, which occurs for an integral over the range of 53° to 127° .

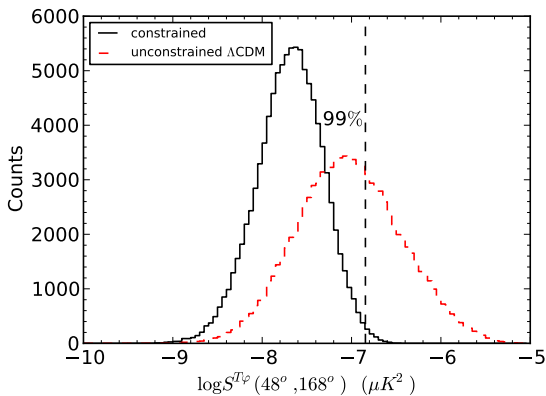


Figure 4. Histogram showing distribution of constrained (black solid) and unconstrained (red dashed) Λ CDM $S_{a,b}^{T\varphi}$ values for $\theta_a = 168^\circ$, $\theta_b = 48^\circ$. This range of angles gives the most optimal statistic for ruling out the null hypothesis at the 99 per cent level.

null hypothesis by investigating which pair of angles used in calculating $S_{a,b}^{T\varphi}$ defined in Eq. 13 provided the largest percentage of unconstrained Λ CDM $S_{a,b}^{T\varphi}$ lying above the 99-per centile value for the constrained distribution. We find that restricting the integration range from 48° to 168° slightly improves the ability of the statistic to rule out a given measured value being consistent with constrained Λ CDM. To rule out the fluke hypothesis at the 99.9-per centile level, we found that the optimal range of angles is 53° to 130° . The contours showing the discriminating power of the $S_{a,b}^{T\varphi}$ statistic for the constrained Λ CDM versus unconstrained Λ CDM were shown in Figs. 2 and 3, and the histograms for the $S_{a,b}^{T\varphi}$ statistic for the optimal angular ranges were shown in Figs. 4 and 5. However, because the improvement over the $S_{1/2}^{T\varphi}$ statistic is modest, and because $S_{a,b}^{T\varphi}$ is optimized to select between con-

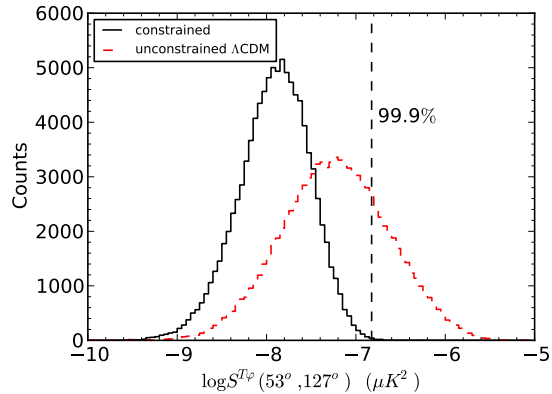


Figure 5. Histogram showing distribution of constrained (black solid) and unconstrained (red dashed) Λ CDM $S_{a,b}^{T\varphi}$ values for $\theta_a = 127^\circ$, $\theta_b = 53^\circ$. This range of angles gives the most optimal statistic for ruling out the null hypothesis at the 99.9 per cent level.

strained Λ CDM and unconstrained Λ CDM, simplicity argues for using $S_{1/2}^{T\varphi}$ to parallel previous analysis of C_ℓ^{TT} .

The outlined procedure for assessing the discriminating power of the $T\varphi$ cross-correlation statistics can be used as a generic prescription for optimizing statistics of any cosmological data. Choice of a particular confidence level to optimize for should always be made before calculations of any $S_{1/2}$ -like statistics are carried out to avoid any bias in reporting results.

Clearly, some model comparisons will provide statistics from $T\varphi$ that are more useful than others. In particular, since the φ field is dominated by effects inside the last-scattering surface, it has a large correlation with Θ_{ISW} . This means that unless a proposed model can find some way to suppress this particular term, there will not be a sharp difference for $S_{a,b}^{T\varphi}$ statistics from Λ CDM, which will limit its usefulness if one prefers to compare their model to Λ CDM. Regardless, $T\varphi$ correlations will provide an important consistency check for the data, as the large $\Theta_{\text{ISW}}\varphi$ contribution is a probe of physics on the interior of our Hubble volume. It is therefore complimentary to the TT signal which is largely comprised of effects at the last-scattering surface.

The $S^{T\varphi}$ statistic is not particularly helpful for testing a hypothesis that the underlying gravitational potential fluctuations lack correlations on scales larger than some comoving scale subtending 60° at the redshift of last scattering. Any suppression in $\langle \Phi(\hat{n}_1)\Phi(\hat{n}_2) \rangle$ that gives rise to the observed TT spectrum would *not* have any significant effect on the shape of $C^{T\varphi}(\theta)$ compared to Λ CDM. This fact is precisely due to the large $\Theta_{\text{ISW}}\varphi$ term.

Other cross correlations may prove to be more fruitful. For example, 21 centimeter emission correlated with temperature fluctuations will partially mitigate the large $\Theta_{\text{ISW}}\varphi$ problem. The 21 centimeter emission spectrum comes to us from localized region of redshift space, and does not have a component which is an integral along the line of sight. This in particular should reduce the magnitude of the correlation compared to $C^{T\varphi}(\theta)$. In a future work, we will show how viable this cross correlation will be for testing the null hypothesis, as well as provide predictions for the shape of $C(\theta)^{T 21\text{cm}}$ with an imposed cutoff.

A related calculation (Copi 2013a) examined the implications of the fluke hypothesis for the temperature-polarization angular correlation function, in particular the correlation of temperature with the Stokes Q parameter, $C^{TQ}(\theta)$. This statistic excludes the fluke hypothesis at 99.9 per cent C.L. for 26 per cent of realizations of unconstrained Λ CDM, or at 99 per cent C.L. for 39 per cent of such realizations.

In summary, the temperature auto-correlation of the CMB sky behaves oddly at large angular separations. No satisfactory current theory explains this anomaly, and so the leading explanation is that it is a statistical fluke. In the absence of specific models to compare directly with Λ CDM, the best strategy is to identify other measurable quantities with probability distributions that are affected by the knowledge that $S_{1/2}^{TT}$ is small, and make predictions for the new probability distribution functions. In this way we can test the fluke hypothesis with current and near-future CMB data sets.

ACKNOWLEDGEMENTS

The authors would like to thank Simone Aiola for useful discussions. The numerical simulations were performed on the facilities provided by the Case ITS High Performance Computing Cluster. AY is supported by NASA NESSF Fellowship. CJC, GDS and AY are supported by a grant from the US DOE to the Particle Astrophysics Theory group at CWRU. AK has been partly supported by NSF grant AST-1108790.

REFERENCES

- Ade P. A. R. et al., [Planck Collaboration], [arXiv:1303.5083].
 Bennett C. L., Banday A., Gorski K. M., Hinshaw G., Jackson P., Keegstra P., Kogut A., Smoot G. F. et al., *Astrophys. J.* 464, L1 (1996) [astro-ph/9601067].
 Chang Z., Wang S., *Eur. Phys. J. C*, 73:2516 (2013) [arXiv:1303.6058].
 Copi C. J., Huterer D., Starkman G. D., *Phys. Rev. D* 70, 043515 (2004)
 Copi C. J., Huterer D., Schwarz D. J., Starkman G. D., *Mon. Not. Roy. Astron. Soc.* 367, 79 (2006) [astro-ph/0508047].
 Copi C. J., Huterer D., Schwarz D. J., Starkman G. D., *Phys. Rev. D* 75, 023507 (2007) [astro-ph/0605135].
 Copi C. J., Huterer D., Schwarz D. J., Starkman G. D., *Mon. Not. Roy. Astron. Soc.* 399, 295 (2009) [arXiv:0808.3767].
 Copi C. J., Huterer D., Schwarz D. J., Starkman G. D., *Adv. Astron.* 2010, 847541 (2010) [arXiv:1004.5602].
 Copi C. J., Huterer D., Schwarz D. J., Starkman G. D., 2013, preprint [arXiv:1303.4786].
 Copi C. J., Huterer D., Schwarz D. J., Starkman G. D., arXiv:1310.3831 [astro-ph.CO].
 de Oliveira-Costa A., Tegmark M., Zaldarriaga M., Hamilton A., *Phys. Rev. D* 69, 063516 (2004) [astro-ph/0307282].
 Efstathiou G., Ma Y. Z., Hanson D., [arXiv:0911.5399].
 Eriksen H. K., Banday A. J., Gorski K. M., Hansen F. K., Lilje P. B., *Astrophys. J.* 660, L81 (2007) [astro-ph/0701089].
 Gorski K. M., Hivon E., Banday A. J., Wandelt B. D., Hansen F. K., Reinecke M., Bartelman M., *Astrophys. J.* 622, 759 (2005) [astro-ph/0409513].
 Hinshaw G., Banday A. J., Bennett C. L., Gorski K. M., Kogut A., Lineweaver C. H., Smoot G. F., Wright E. L., *Astrophys. J.* 464, L25 (1996) [astro-ph/9601061].
 Hou Z., Banday A. J., Gorski K. M., [arXiv:0903.4446].
 Land K., Magueijo J., *Phys. Rev. Lett.* 95, 071301 (2005) [astro-ph/0502237].
 Lewis A., Challinor A., Lasenby A., *Astrophys. J.* 538, 473 (2000) [astro-ph/9911177].
 Liu H., Frejsel A. M., Naselsky P., *JCAP* 1307, 032 (2013) [arXiv:1302.6080].
 Lyth D. H., *JCAP* 1308, 007 (2013) [arXiv:1304.1270].
 Pontzen A., Peiris H. V., *Phys. Rev. D* 81, 103008 (2010) [arXiv:1004.2706].
 Schwarz D. J., Starkman G. D., Huterer D., Copi C. J., *Phys. Rev. Lett.* 93, 221301 (2004) [astro-ph/0403353].

Spergel D. N. et al. [WMAP Collaboration], *Astrophys. J. Suppl.* 148, 175 (2003) [astro-ph/0302209].